Supplemental Materials

Methods

A bivariate correlation table is presented in table S1. Figure S1 depicts participant recruitment across study waves. Figure S2 depicts the emotion regulation task used.

Image Acquisition

Scanning was performed on a 3T Siemens Trio scanner at the Harvard Center for Brain Science using a 32-channel head coil. Anatomical scans (T1-weighted multi-echo MPRAGE volumes; TR=2530ms, TE=1640-7040μs, flip angle=7°, FOV=220mm^2, 176 slices, in-plane voxel size=1mm3) were acquired for co-registration with functional magnetic resonance imaging (fMRI). To reduce motion-related artifacts slices were compared to a navigator echo acquired prior to the anatomical scan and up to 20% of slices were allowed to be re-acquired in response to participant motion.

Blood oxygenation level dependent (BOLD) signal during functional runs was acquired using a gradient-echo T2*-weighted echo planar imaging (EPI) sequence. Thirty-two 3mm thick slices were acquired parallel to the anterior and posterior commissure (AC-PC) line (TR=2500ms, TE=30ms, flip angle=90°, bandwidth=2240Hz/px, echo spacing=0.51, FOV=216mm^2, matrix size=72x72). Prior to each scan, four images were acquired and discarded to allow longitudinal magnetization to reach equilibrium. An online prospective motion correction algorithm (PACE) was used to reduce the effect of motion artifacts.

Image Pre-Processing

Preprocessing and analysis steps were implemented within GNU Make, a tool designed for building software from source files that can be used to create neuroimaging workflows incorporating multiple software packages (Askren et al., 2016). Freesurfer version 5.3 was used to calculate brain surfaces and WM/CSF masks; Freesurfer volumes were inspected and hand-edited to remove artifacts (Fischl et al., 2002). Anatomical co-registration of the functional data with each participant's T1-weighted image was performed using surface-based registration in FreeSurfer, which provides better alignment

than other methods in children (Ghosh et al., 2010). Functional volumes were simultaneously motion and slice timing corrected (Roche, 2011). Skull stripping was performed using OptiBET (Lutkenhoff et al., 2014) and BET (Smith, 2002) in FSL (Jenkinson, Beckmann, Behrens, Woolrich, & Smith, 2012). Volumes were despiked using AFNI's 3dDespike tool (Cox, 1996) and smoothed using a 6mm full-width half-max kernel in FSL using SUSAN (Smith & Brady, 1997). 6 rigid-body motion regressors were included in person-level models. High-motion volumes (of 1 voxel or greater) or volumes where the derivative of variance in BOLD signal across the brain (DVARS) exceeded the upper fence (above 75th percentile + 1.5 × inter-quartile range) or the change in signal intensity exceeded 3 SD were considered outliers and excluded from analysis by regressing these volumes out of person-level models. No significant differences were found between abused and control participants on any motion parameter (all $p<.21$). Time series extracted from white matter and ventricles generated using FreeSurfer and FSL were additionally controlled for in the person-level models to control for physiological noise (Behzadi, Restom, Liau, & Liu, 2007). Following estimation of person-level models, the resulting contrast images were registered to standard space of the Montreal Neurological Institute template. All normalization was implemented in Advanced Normalization Tools (ANTs) software (Avants et al., 2011).

Results

Functional connectivity during regulation

We additionally examined task-related functional connectivity in the decrease negative > look negative contrast (ie. functional connectivity correlated with participant's efforts to actively regulate negative emotion). No clusters survived cluster level correction in this analysis.

Functional connectivity during stimulus exposure

We conducted a post-hoc analysis to examine whether differences in task-related functional connectivity in the look negative > look neutral contrast were driven by differences in response to negative or neutral images specifically. Two new PPI analyses were run using the same methods as the

primary analysis, but substituting the contrast regressor for a look negative only (> baseline) and a look neutral only regressor, respectively. These models produced estimates of functional connectivity to left amygdala during exposure to stimuli of each valence while controlling for baseline connectivity. Region of interest analyses were repeated in these models for both vmPFC ROIs. 2×2 ANOVA models were run to examine main effects of valence, group, and their interaction on task-related functional connectivity while controlling for age, race, sex, and parent education.

A significant interaction between abuse and contrast was detected for both sgACC ($F(1,54)=14.12$, $p<.001$) and mOFC ($F(1,54)=5.77$, $p=.02$). Tukey HSD tests were run to detect pair-wise differences. In both ROIs, connectivity to amygdala while viewing negative stimuli was more negative than connectivity while viewing neutral stimuli in adolescents exposed to child abuse. Tests for differences between groups showed that adolescents exposed to child abuse showed a trend towards more negative connectivity between sgACC and left amygdala to negative stimuli (over baseline) vs. control adolescents ($p=.1$), as well as a trend toward more positive connectivity to neutral stimuli ($p=.091$). These associations are illustrated in figure S3.

Association of exposure variables with task related functional connectivity.

We re-ran models examining the association of abuse, community violence, and parent education with task related functional connectivity after controlling for concurrent psychopathology. Associations of task related functional connectivity between left amygdala and mOFC with abuse became non-significant in this analysis, but association of task related functional connectivity between left amygdala and sgACC remained (see table S2).

References

Askren, M. K., McAllister-Day, T. K., Koh, N., Mestre, Z., Dines, J. N., Korman, B. A., … Madhyastha, T. M. (2016). Using make for reproducible and parallel neuroimaging workflow and quality-assurance. *Frontiers in Neuroinformatics*, *10*, 2. https://doi.org/10.3389/fninf.2016.00002

Avants, B. B., Tustison, N. J., Song, G., Cook, P. A., Klein, A., & Gee, J. C. (2011). A reproducible evaluation of ANTs similarity metric performance in brain image registration. *NeuroImage*, *54*(3), 2033–2044. https://doi.org/10.1016/j.neuroimage.2010.09.025

Behzadi, Y., Restom, K., Liau, J., & Liu, T. T. (2007). A component based noise correction method (CompCor) for BOLD and perfusion based fMRI. *NeuroImage*, *37*(1), 90–101. https://doi.org/10.1016/j.neuroimage.2007.04.042

Cox, R. W. (1996). AFNI: software for analysis and visualization of functional magnetic resonance neuroimages. *Computers and Biomedical Research*, *29*(3), 162–173. https://doi.org/10.1006/cbmr.1996.0014

Fischl, B., Salat, D. H., Busa, E., Albert, M., Dieterich, M., Haselgrove, C., … Dale, A. M. (2002). Whole brain segmentation: automated labeling of neuroanatomical structures in the human brain. *Neuron*, *33*(3), 341–355.

Ghosh, S. S., Kakunoori, S., Augustinack, J., Nieto-Castanon, A., Kovelman, I., Gaab, N., … Fischl, B. (2010). Evaluating the validity of volume-based and surface-based brain image registration for developmental cognitive neuroscience studies in children 4-to-11 years of age. *NeuroImage*, *53*(1), 85–93. https://doi.org/10.1016/j.neuroimage.2010.05.075

Jenkinson, M., Beckmann, C. F., Behrens, T. E. J., Woolrich, M. W., & Smith, S. M. (2012). FSL. *NeuroImage*, *62*(2), 782–790. https://doi.org/10.1016/j.neuroimage.2011.09.015

Lutkenhoff, E. S., Rosenberg, M., Chiang, J., Zhang, K., Pickard, J. D., Owen, A. M., & Monti, M. M. (2014). Optimized brain extraction for pathological brains (optiBET). *PLOS ONE*, *9*(12), e115551. https://doi.org/10.1371/journal.pone.0115551

Roche, A. (2011). A four-dimensional registration algorithm with application to joint correction of motion and slice timing in fmri. *IEEE Transactions on Medical Imaging*, *30*(8), 1546–1554. https://doi.org/10.1109/TMI.2011.2131152

Smith, S. M. (2002). Fast robust automated brain extraction. *Human Brain Mapping*, *17*(3), 143–155. https://doi.org/10.1002/hbm.10062

Smith, S. M., & Brady, J. M. (1997). SUSAN—a new approach to low level image processing. *International Journal of Computer Vision*, *23*(1), 45–78. https://doi.org/10.1023/A:1007963824710

Tables

Supplemental Table 1: Correlations between study variables.

Measure	*1*	*2*	*3*	*4*	*5*	*6*	*7*	*8*
1. Age at Scan	–							
2. Sex	-.13	–						
3. Combined Abuse	.00	.12	–					
4. Parent Ed.	-.14	.13	-.09	–				
5. Comm. Violence	.14	-.21	.14	-.46**	–			
6. Internalizing (Wave 2)	-.03	.04	.61**	.02	.19	–		
7. Externalizing (Wave 2)	.07	-.21	.50**	-.16	.48**	.64**	–	
8. Internalizing (Wave 3)	-.24	.28	.50**	.11	.09	.67**	.33*	–
9. Externalizing (Wave 3)	-.17	.02	.39*	-.14	.39*	.35*	.58**	.52**

*: $p<.05$
**: $p<.001$

Supplemental Table 2: Association of exposure variables with task related functional connectivity controlling for concurrent psychopathology.

	L. Amyg × mOFC			R.Amyg × mOFC			L. Amyg × sgACC			R.Amyg × sgACC		
Threat:	*F*	*η2*	*p*	*F*	*η2*	*p*	*F*	*η2*	*p*	*F*	*η2*	*p*
Abuse	.72	.01	.402	0	0	.98	8.53*	.13	.005	1	.02	.323
Community Violence	.24	0	.628	1.30	.02	.26	.68	.01	.415	1.65	.03	.206
	B		*P*	*B*		*P*	*B*		*P*	*B*		*p*
Abuse Severity	-.3		.077	-.15		.43	-.48*		.006	-.19		.313
Community Violence Severity	-.07		.702	-.31		.13	-.17		.387	-.26		.200
SES:	*F*	*η2*	*p*	*F*	*η2*	*p*	*F*	*η2*	*p*	*F*	*η2*	*p*
Less than College Degree	1.35	.02	.252	.14	0	.72	3.00	.04	.090	.5	.01	.482
	B		*p*	*B*		*P*	*B*		*P*	*B*		*P*
Parent Education	.15		.261	-.07		.64	.16		.258	.04		.775

*: $p<.05$

**: $p<.001$

All models controlled for age, race, sex, and concurrent psychopathology. Threat models controlled for parent education and vice versa.

Figures

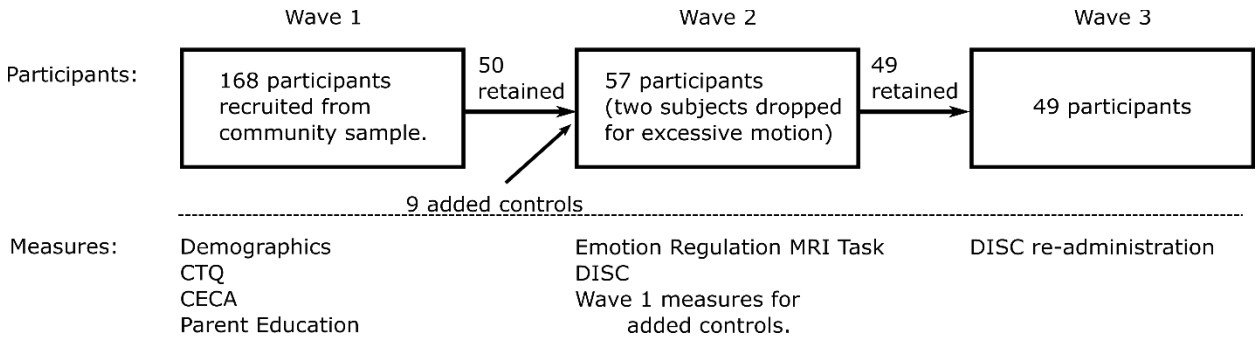

Supplemental Figure 1: Study Flow Diagram

Supplemental Figure 2: Emotion regulation task. The average valence and arousal of images and the number of faces within each image were equivalent for trials using negative stimuli (look and decrease) and trials using positive stimuli (look and increase). The instructional cue appeared for 2 seconds, the emotional stimulus appeared for 6 to 10 seconds, the rating screen appeared for 4 seconds, and the intertrial interval (ITI) lasted from 1.5 to 6.5 seconds. The emotional stimulus and ITI were jittered by sampling durations in the following manner: 50% of the shortest, 25% of the middle duration, and 25% of the longest duration.

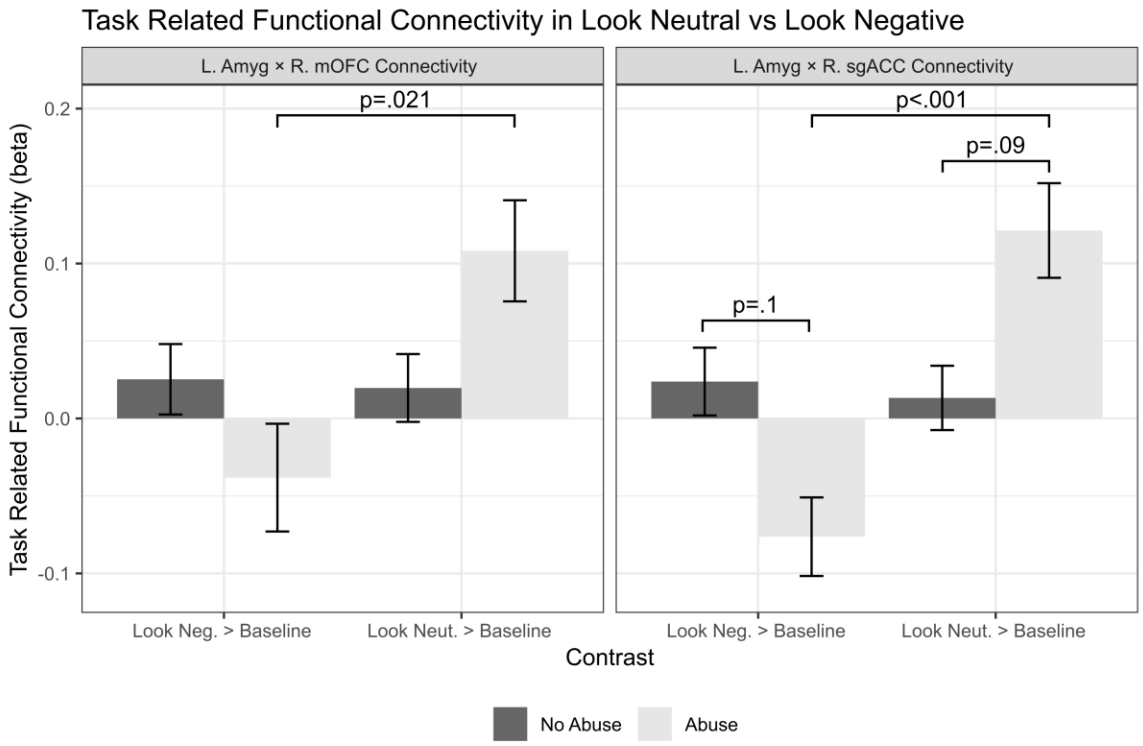

Supplemental Figure 3: Task-related functional connectivity vs. baseline in adolescents by group.